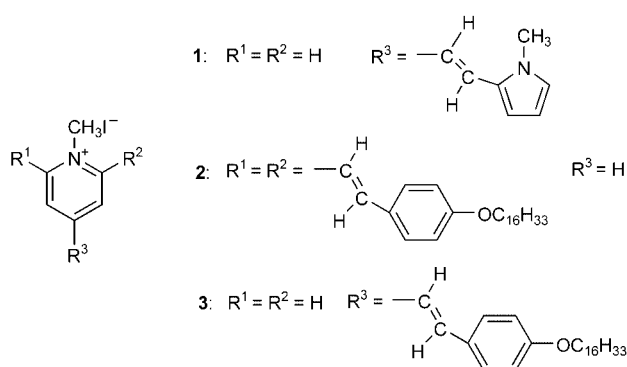


Low-Dimensional Aggregates from Stilbazolium-Like Dyes\*\*

Zhiyuan Tian, Yu Chen, Wensheng Yang, Jiannian Yao,\*  
Lingyun Zhu, and Zhigang Shuai

Organic low-dimensional nanostructures used as nanoscale building blocks have attracted considerable research interest in the development of novel nanodevices.<sup>[1]</sup> This interest is driven by the fact that organic nanostructures may exhibit a wide range of electrical and optical properties that depend sensitively on both their shapes and sizes, and thus is likely to provide a new method for modifying the optical and electronic properties of organic functional materials.<sup>[2]</sup> From this standpoint, an important challenge in the discovery of novel mesoscopic properties and the development of nanotechnology is to fabricate organic nanomaterials with the desired shape and size. Although extensive studies on the size-dependent optical and electronic properties of organic nanostructures such as particles,<sup>[2a-d]</sup> wires,<sup>[2e]</sup> and tubes<sup>[2f]</sup> have been performed recently, the ability to understand and predict the final structures of nanomaterials, which is critical to guide the rational fabrication of nanoscale materials with a desired shape, size, and therefore function, is still limited.<sup>[2a,3]</sup>

Herein, we report the facile fabrication of organic nanostructures with well-defined shapes and uniform sizes from stilbazolium-like dyes (Scheme 1). Compounds 1–3 were synthesized with the original intention of exploring the possible influence of the substituents on the shape, and therefore the optical properties, of the resulting nanostructures. Low-dimensional nanorods and nanospheres with high monodispersities in both shape and size were prepared by the self-aggregation of compounds 1 and 2, respectively. The concomitant property changes upon formation of nanorods with intermolecular charge-transfer (inter-CT) characteristics, as well as highly monodisperse nanospheres with size-dependent spectral features, may be exploited in many fields.<sup>[1b]</sup>



Scheme 1. Structures of model compounds 1–3.

The aggregation of molecule 1 was induced by injecting a certain amount of stock solution of compound 1 in ethanol into a 1:1 mixed solvent of hexane and methylcyclohexane (MCH) with vigorous stirring. Ethanol is a good solvent but the mixed solvent is a poor one for compound 1, so aggregation of molecule 1 occurred as a consequence of the change in the solvent quality. The size of nanostructures of 1 was controlled by varying the concentration of the stock solution. For example, nanorod sizes of 110 and 80 nm were obtained when 60  $\mu\text{L}$  of the  $1.0 \times 10^{-3}$  M stock solution and 120  $\mu\text{L}$  of the  $5.0 \times 10^{-4}$  M stock solution were injected, respectively. Water was used as the poor solvent for the aggregation of compound 2 to obtain the colloids. The average size of nanostructures of 2 was controlled through a ripening process by variation of the aging time, that is, by changing the time intervals after injection of the stock solution. For example, aging times of 15 and 30 minutes gave nanospheres with diameters of 60 and 100 nm, respectively. The nanorods obtained from compound 1 and the nanospheres from compound 2 were very uniform in size, as indicated by the scanning (SEM) and tunneling electron microscopy (TEM) images (Figure 1). It can be seen that the sample derived from 1 consists of rather straight nanorods

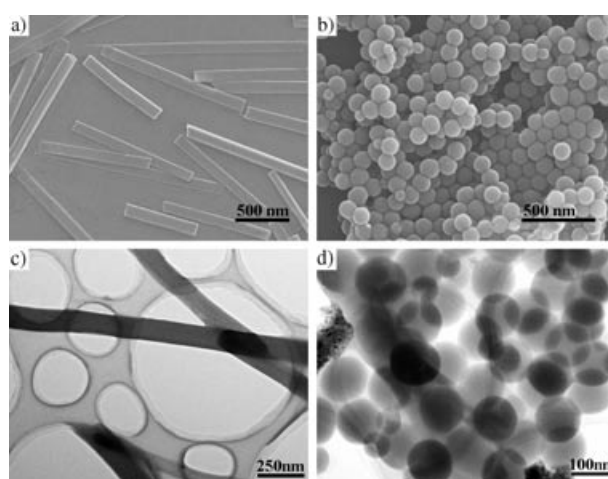


Figure 1. a) Medium-magnification SEM images of the nanorods formed from 1. b) Low-magnification SEM images showing a large quantity of the nanospheres formed from 2. c) TEM image of the nanorods. d) TEM image of the nanospheres.

[\*] Dr. Z. Tian, Y. Chen, W. Yang, Prof. J. Yao  
Key Laboratory of Photochemistry  
Center for Molecular Science  
Institute of Chemistry, Chinese Academy of Sciences  
Beijing 100080 (P. R. China)  
Fax: (+86) 10-8261-6517  
E-mail: jnyao@mail.iccas.ac.cn

Dr. L. Zhu, Prof. Z. Shuai  
Key Laboratory of Organic Solids  
Center for Molecular Science  
Institute of Chemistry, Chinese Academy of Sciences  
Beijing 100080 (P. R. China)

[\*\*] This work was supported by the National Natural Science Foundation of China, the Chinese Academy of Sciences, and the National Research Fund for Fundamental Key Projects No.973 (G19990330).

Supporting information for this article is available on the WWW under <http://www.angewandte.org> or from the author.

with lengths up to the micrometer range that have a uniform size along the entire length. In addition, the surfaces of the nanorods are clean and smooth. The product from **2** consists of a large quantity of perfect nanospheres with very high monodispersity in terms of size, and some nanospheres are assembled into regular hexagonal arrays in a small domain (see Supporting Information). We note that there are scarcely any previous examples of nanostructures with such high monodispersity from small organic molecules without the use of templates. Furthermore, the distinct morphological features as well as the high monodispersity in size of the nanostructures of **1** and **2** lead us to assume that there would, most probably, be specific driving forces involved in the formation of these nanostructures.

It is known that the spectra of the nanostructures can give information about the formation process.<sup>[2a-e]</sup> Figure 2 displays the absorption spectra of the colloidal dispersions of the as-prepared nanorods and nanospheres. The monomer of **1** in ethanol exhibits an intensive intramolecular charge-transfer (intra-CT) absorption band at about 446 nm (2.77 eV), which is assigned to the transition from the HOMO of the donor to the LUMO of the acceptor (that is,  $\pi_D-\pi_A^*$ ).<sup>[4]</sup> In the spectra of nanorods of **1**, the intra-CT band shows a slight gradual red

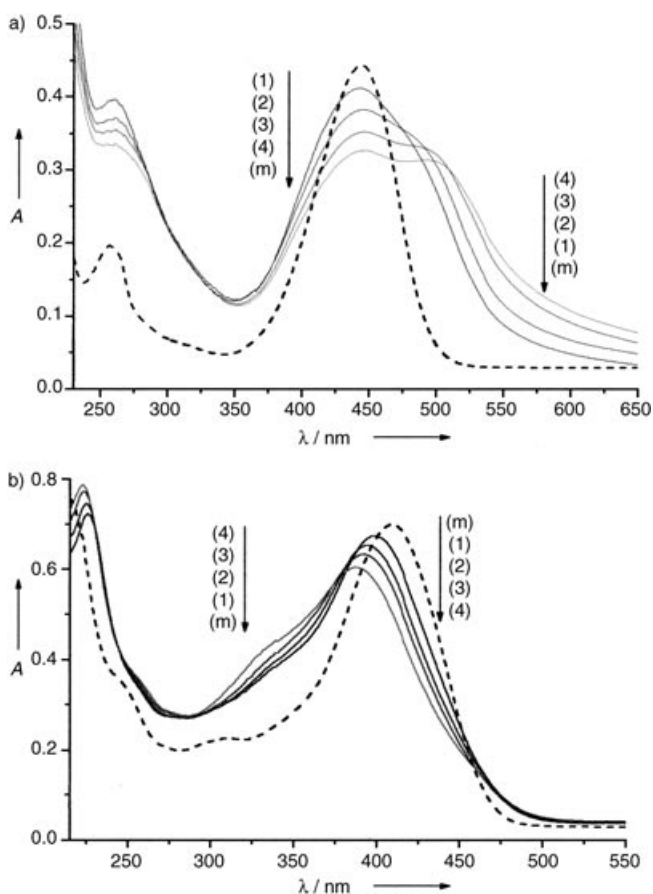


**Figure 2.** a) Absorption spectra of dispersions of nanorods with different diameters: 1) 40 nm, 2) 80 nm, 3) 110 nm, 4) 150 nm. b) Absorption spectra of dispersions of nanospheres with different sizes: 1) 30 nm, 2) 60 nm, 3) 100 nm, 4) 130 nm. For comparison, the spectra of the corresponding monomers in ethanol are also shown as (m) in (a) and (b) (dashed lines). A = absorbance (arbitrary units).

shift with increasing nanorod size and simultaneously an additional band centered at approximately 500 nm (2.48 eV) emerges and gradually becomes predominant at the expense of the intra-CT band. This new band is attributed to an inter-CT transition between neighboring molecules in the nanorods.<sup>[1a]</sup> The spectrum of dilute **2** in ethanol solution also exhibits an intensive  $\pi-\pi^*$  band at about 409 nm (3.03 eV), while the spectra of the nanospheres shift gradually to shorter wavelengths on increasing the particle size. In addition, both the excitation and emission fluorescence spectra of the nanospheres show similar hypsochromic shifts as the absorption spectra (see Supporting Information). However, only very weak fluorescence emission was detected for the nanorods of **1**, which indicates that strong quenching occurred in the aggregates of model molecule **1**.

Molecule **1** consists of a strong electron-withdrawing moiety *N*-methylpyridinium (Nmpd) and a strong electron-releasing moiety *N*-methylpyrrole (Nmpr) connected by a conjugated system.<sup>[5]</sup> For molecule **2**, two weak electron-releasing 4-hexadecyloxyphenyl (4Hop) moieties, relative to Nmpr, are symmetrically connected to the Nmpd moiety through a conjugated ethylene group. One noteworthy conformational difference between molecules **1** and **2** is the planarity: the dihedral angles  $\theta$  between the  $\pi$  systems of the donor and acceptor groups are nearly  $0^\circ$  for molecule **1** but  $33^\circ$  for molecule **2**, as indicated by the molecular mechanics optimizations of single molecules of **1** and **2** (Figure 3 a,b). It can also be seen from Figure 3 that molecule **1** has a linear D- $\pi$ -A structure, while this is not the case for **2**. These molecular structural and conformational differences are expected to be responsible for the different spectral features, such as the 0.26 eV difference in the  $\pi-\pi^*$  transition energy between monomers **1** and **2** that reflects the different extent of  $\pi$ -electron delocalization between the donor and acceptor moieties in the molecules.

SEM and TEM observations, along with the analysis of the molecular structural features and spectroscopic data, provide a clue for the understanding of the possible formation mechanism of the structurally distinct shapes of the nanostructures formed from **1** and **2**. It is well-documented that the spatial configuration of organic molecules plays an important role in determining their stacking mode and therefore the properties of the resulting aggregates.<sup>[2e,6]</sup> For example, an approximately face-to-face arrangement of the donor-acceptor (D-A) pair, which gives the largest orbital overlap, is necessary for the formation of inter-CT complexes. For compounds having the typical molecular structural characteristics of a strong D-A pair, a linear D- $\pi$ -A structure, and a more planar conformation, strong D-A interactions<sup>[7]</sup> are known to act as the main driving force for the aggregation of molecules and the formation of one-dimensional (1D) nanostructures.<sup>[7c]</sup> The molecular structural characteristics of compound **1** discussed above enabled a similar mechanism to be proposed for the aggregation of molecule **1**, that is, by a donor-to-acceptor growth process (Figure 3c) with eventual formation of rodlike nanostructures. Inter-CT processes<sup>[7c]</sup> and the extended delocalization of  $\pi$  electrons are expected as concomitant spectral features of the strong D-A interactions between adjacent molecules in the nanorods. In fact,

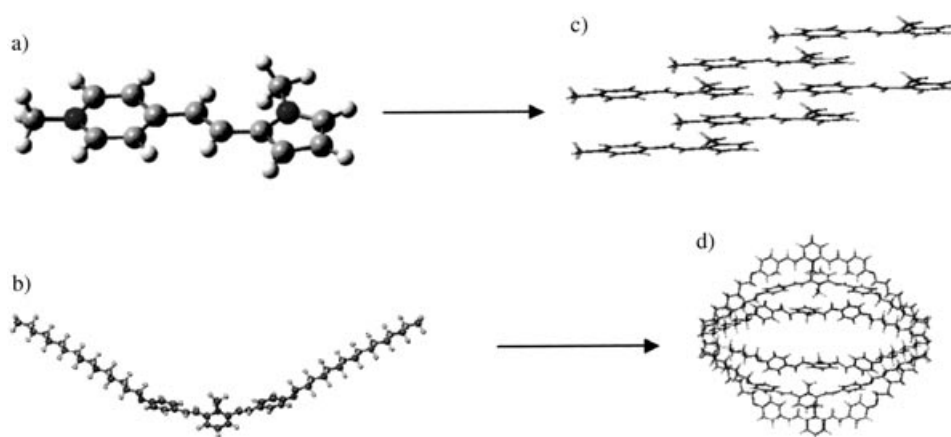


**Figure 3.** Energy-optimized single molecules of **1** (a) and **2** (b); computer-generated 1D aggregates of **1** (c) and 0D aggregates of **2** (d). In Figure 3 d, the length of the hydrocarbon chains was shortened to eight carbon atoms for simplification.

the gradual appearance of a CT band and the slight bathochromic shift of the  $\pi$ - $\pi^*$  band in the spectra are consistent with the proposed mechanism for the formation of the nanorods. In addition, the quenching of the nanorod fluorescence emission can also be attributed to the presence of low-lying CT states in the nanorods.<sup>[8]</sup> XRD measurements show that the nanorods grow preferentially along the crystallographic [011] direction (see Supporting Information). This kind of preferential growth along a specific crystallographic direction is prone to forming 1D structures.

In the case of **2**, however, the possibility of D–A interaction acting as the dominating driving force for the aggregation of molecules was excluded because of the weak D–A pair, nonlinear molecular structure, and nonplanar configuration, as discussed above. Molecule **2** has two long flexible alkyl side chains substituted on the ionized pyridine ring, and therefore is a typical amphiphilic molecule bearing a hydrophilic “head” (ionized pyridine ring) and two long and flexible hydrophobic “arms” (alkyl chains), as shown in Figure 3b. The gradually blue-shifted spectral characteristics of the nanospheres compared with the monomer suggest the formation of H-type aggregates<sup>[9]</sup> in which the pyridine units are arranged in an almost parallel manner (see Figure 3d). Apparently, this type of aggregation is energetically favorable because it maximizes favorable stacking interactions between pyridine units and minimizes the unfavorable interactions between the molecule and the solvent. Subsequently, these H-type aggregates are presumed to attract each other—this is the so-called collective behavior generally observed in biology and chemistry that originates from interactions between units with the same shape,<sup>[10]</sup> and which is expected to be followed by a process involving fusion and then rearrangement. Nearly the same spectral features (UV/Vis absorption, fluorescence emission and excitation) as those discussed above, as well as spherical nanostructures, were observed when the mixed solvent of 1:1 hexane/MCH was used as the poor solvent during the aggregation of **2**. This finding indicates that it is mainly the difference between the compatibility of the two moieties (4Hop and Nmpd) of molecule **2** with the poor solvent, as well as the specific molecular structural features, that eventually lead to the

aggregation of molecule **2** in a manner different from that of molecule **1**. Somewhat surprisingly, the nanospheres obtained after the ripening process are very monodisperse both in terms of shape and size (Figure 1b and Supporting Information). Similar results were also obtained in our previous work concerning organic nanostructures derived from pyrazoline derivatives.<sup>[2c,d]</sup> As discussed above, the growth of the nanospheres appears to be involved in the process consisting of the attraction, fusion, and rearrangement of relatively small particles, which suggests that the Ostwald ripening mechanism most probably does not apply to the present case. The relatively small particles are expected to aggregate preferentially through solvophobic interactions and then fuse as a result of their relatively large surface areas, eventually giving the focused size distribution of the nanospheres produced.<sup>[11]</sup> The underlying basis of the narrow size distribution of the as-prepared nanostructures is still under investigation.

Molecular modeling studies also provide a coherent picture of the process by which the resulting nanostructures are formed. The spectral features generated from the proposed aggregation models, namely the slight red shift of the intra-CT band and the inter-CT process between adjacent molecules in nanorods of **1**, as well as the blue-shifted intra-CT transition in the nanospheres of **2**, agree well with our experimental results. In particular, the calculated results clearly show the charge-transfer process from the donor to acceptor units between neighboring molecules in the case of nanorods (see Supporting Information).

The morphological and spectral features of the nanostructures formed by reference model compound **3** were also investigated. Molecule **3** is found to aggregate into rodlike nanostructures, as indicated by SEM studies (see Supporting Information). Although molecule **3** has a linear structure, it has a weak D–A interaction between the Nmpd and 4Hop moieties compared to molecule **1**, and thus may aggregate in a head-to-tail fashion through intermolecular D–A interactions, which should be much weaker than those occurring within the rods. However, molecule **3** bears only one long flexible alkyl chain while two are present in molecule **2**. Thus, the solvophobic interaction is unlikely to result in the formation of H-type aggregates with a nearly parallel

arrangement of the pyridine ring moieties of molecule **3**. As a result, neither the apparent inter-CT feature similar to that observed in the spectra of the nanorods nor the gradually blue-shifted spectral feature on increasing the particle size, seen in the spectra of the nanospheres, is observed for the rodlike nanostructures in our experiments (see Supporting Information). The morphology of aggregates from **3** is relatively undefined compared to that of the rods and particles as a result of competition between the two relatively weaker D–A and solvophobic interactions.

In conclusion, we have successfully prepared stilbazolium-like dye nanorods and nanospheres by changing the solvent quality during the synthesis of model compounds. Sufficiently strong interactions between the constituent molecules allow the formation of nanostructures with well-defined shape and highly monodisperse size. Furthermore, different dominant intermolecular interactions, based on molecular components with different structural and conformational characteristics, are likely to be responsible for the formation of organic nanostructures with distinct shapes. This work provides specific examples and, therefore, the possibility of constructing nanomaterials that are expected to be useful in the development of photoelectronic nanodevices.

Received: February 27, 2004 [Z54131]

**Keywords:** aggregation · charge transfer · donor–acceptor systems · nanostructures · solvophobic interaction

- [1] a) S. R. Forrest, *Chem. Rev.* **1997**, *97*, 1793; b) *Handbook of Advanced Electronic and Photonic Materials and Devices, Vol. 6* (Ed.: H. S. Nalwa), Academic Press, San Diego, **2001**.
- [2] a) H. Kasai, H. Kamatani, S. Okada, H. Oikawa, H. Matsuda, H. Nakanishi, *Jpn. J. Appl. Phys.* **1996**, *35*, L221; b) H. B. Fu, J. N. Yao, *J. Am. Chem. Soc.* **2001**, *123*, 1434; c) H. B. Fu, B. H. Loo, D. B. Xiao, R. M. Xie, X. H. Ji, J. N. Yao, B. W. Zhang, L. Q. Zhang, *Angew. Chem.* **2002**, *114*, 1004; *Angew. Chem. Int. Ed.* **2002**, *41*, 962; d) D. B. Xiao, L. Xi, W. S. Yang, H. B. Fu, Z. G. Shuai, Y. Fang, J. N. Yao, *J. Am. Chem. Soc.* **2003**, *125*, 6740; e) H. B. Fu, D. B. Xiao, J. N. Yao, G. Q. Yang, *Angew. Chem.* **2003**, *115*, 2989; *Angew. Chem. Int. Ed.* **2003**, *42*, 2883; f) L. Y. Zhao, W. S. Yang, Y. Ma, J. N. Yao, Y. L. Li, H. B. Liu, *Chem. Commun.* **2003**, 2442.
- [3] a) H. Nakanishi, H. Katagi, *Supramol. Sci.* **1998**, *5*, 289; b) A. Ibanez, S. Maximov, A. Guiu, C. Chaillout, P. L. Baldeck, *Adv. Mater.* **1998**, *10*, 1540; c) J. A. A. W. Elemans, A. E. Rowan, R. J. M. Nolte, *J. Am. Chem. Soc.* **2002**, *124*, 1532.
- [4] M. M. Habashy, F. El-Zawawi, M. S. Antonious, A. K. Sheriff, M. S. A. Abdel-Mottaleb, *Indian J. Chem. Sect. A* **1985**, *24*, 908.
- [5] a) A. Albert, *Heterocyclic Chemistry*, Oxford University Press, New York, **1968**; b) I. D. L. Albert, T. J. Marks, M. A. Ratner, *J. Am. Chem. Soc.* **1997**, *119*, 6575.
- [6] a) M. Pope, C. E. Swenberg, *Electronic Processes in Organic Crystals*, Oxford University Press, Oxford, **1982**; b) C. A. Hunter, J. K. M. Sanders, *J. Am. Chem. Soc.* **1990**, *112*, 5525; c) C. A. Hunter, *Angew. Chem.* **1993**, *105*, 1653; *Angew. Chem. Int. Ed. Engl.* **1993**, *32*, 1584; d) B. K. An, S. K. Kwon, S. D. Jung, S. Y. Park, *J. Am. Chem. Soc.* **2002**, *124*, 14410.
- [7] a) D. B. Amabilino, P. R. Anelli, P. R. Ashton, G. R. Brown, E. Córdova, L. A. Godinez, W. Hanes, A. E. Kaifer, D. Philp, A. M. Z. Slawin, N. Spencer, J. F. Stoddart, M. S. Tolley, D. J. Williams, *J. Am. Chem. Soc.* **1995**, *117*, 11142; b) B. Cabezón, J. G. Cao, F. M. Raymo, J. F. Stoddart, A. J. P. White, D. J. Williams, *Chem. Eur. J.* **2000**, *6*, 2262; c) A. D. L. Escosura, M. V. Martínez-Díaz, P. Thordarson, A. E. Rowan, R. J. M. Nolte, T. Torres, *J. Am. Chem. Soc.* **2003**, *125*, 12300.
- [8] U. Hofstra, R. B. M. Koehorst, T. J. Schaafsma, *Chem. Phys. Lett.* **1986**, *130*, 555.
- [9] E. S. Emerson, M. A. Colin, A. E. Rosenoff, K. S. Norland, H. Rodriguez, D. Chin, G. R. Bird, *J. Phys. Chem.* **1967**, *71*, 2396.
- [10] a) M. Adams, Z. Dogic, S. L. Keller, S. Fraden, *Nature* **1998**, *393*, 349; b) V. J. Anderson, H. N. W. Lekkerkerker, *Nature* **2002**, *416*, 810; c) Z. Y. Tang, N. A. Kotov, M. Giersig, *Science* **2002**, *297*, 237.
- [11] a) X. G. Peng, J. Wickham, A. P. Alivisatos, *J. Am. Chem. Soc.* **1998**, *120*, 5343; b) Z. A. Peng, X. G. Peng, *J. Am. Chem. Soc.* **2001**, *123*, 1389.